Establishment and Origin of Two-temperature X-ray Plasma from Pre-main-sequence Stars

Tsujimoto, M.[1], Koyama, K.[2], & Tsuboi, Y.[3]
[1]Pennsylvania State University, [2]Kyoto University, [3]Chuo University
<tsujimot@astro.psu.edu>

1. Introduction

X-ray observations on pre-main-sequence (PMS) stars have mainly focused on low-mass sources (0.2-2.0M_o) in the past. Their X-ray spectra of these sources are explained by T=5-50 MK thin-thermal plasma emissions and the light curves often show flare-like variability of fast rise and slow decay. These characteristics are similar to the Sun, hence the X-ray emissions from low-mass PMS stars are explained in the solar analogue; i.e., X-rays originate from the plasma maintained by occasional magnetic reconnections.

This poster aims to address the following two questions;

(1) Do PMS stars with different mass ranges (M >2.0 M_o or M <0.2M_o) have X-ray emissions? The paucity of intermediate-mass (IM; 10.0M_o>M >2.0M_o) and the faintness of very-low-mass (VLM; M <0.2M_o) PMS samples made it difficult to study this issue with the previous satellites.

(2) Can the X-ray emissions from PMS stars explained by flares alone? Why do they have X-ray emissions in quiescent phases (Fig.1)? Also, the plasma temperature is about 10 times higher in PMS stars than in the Sun. What does this implicate?

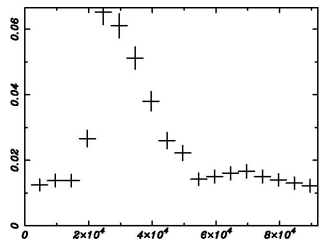

Fig.1 A typical light curve (time [s] vs X-ray count rate [1/s]) of PMS stars.

2. Observation

Selecting Orion Molecular Cloud 2 and 3 (OMC-2/3) as our study field, we conducted an X-ray imaging-spectroscopy observation (0.5-8 keV) using *Chandra* / ACIS-I and a NIR imaging observation (J, H, K) using the University of Hawaii 88-inch telescope / QUIRC. From the X-ray image, 385 sources were extracted at F_x>$10^{-15.5}$ ergs/s/cm^2, while from the NIR image 1448 sources were detected at K <16.0 mag.

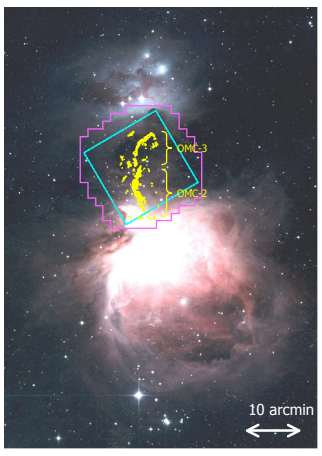

Fig.2 Optical image of the Orion Nebula (courtesy: Kiso Observatory, the University of Tokyo). The FOVs of ACIS-I and QUIRC are shown with cyan and magenta lines. The yellow contours are 1.3 mm intensity[1].

3. Analysis

3.1. NIR Identification

Among 385 X-ray sources, 203 were identified with the 2MASS sources (K_s <14.3 mag). The remaining 182 X-ray sources were correlated with our QUIRC data and 75 were identified with the QUIRC sources. In total, 72% (278/385) X-ray sources were identified with the NIR sources.

The X-ray sources with significant J- and H-band detections (268 sources) were plotted on the color-magnitude diagram (Fig.3) to estimate their mass. We divided them into four mass ranges; High-mass (HM; M >10M_o), intermediate-mass (IM; 10M_o >M > 2M_o), low mass (LM; 2M_o >M >0.2M_o), and very low mass (VLM; M < 0.2M_o).

We also divided all the NIR sources into four mass ranges in the same manner and derived the X-ray detection rate of each mass range (Table 1).

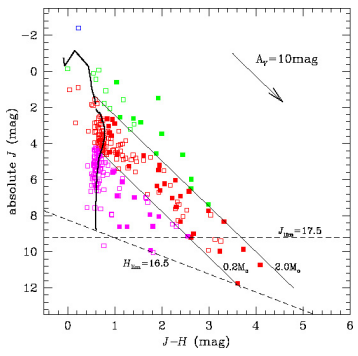

Fig.3 J/(J-H) color-magnitude diagram. The NIR-identified X-ray sources are plotted with blue (HM), green (IM), red (LM), and magenta (VLM) colors. Filled are those with NIR excess. The 1 Myr iso-chrone curves are given in thick solid lines (4.0–1.4M_o [2] and 1.4–0.002M_o [3]).

3.2. X-ray Temporal Analysis

120 X-ray sources with (1) S/N >10 and (2) X-ray counts > 200 were fitted with a constant flux model. 66 of them, which were rejected with this model with a 1% significance level, were labeled as "variable".

Table 1 X-ray detection rate of each mass range.

Mass range (M_o)	HM >10	IM 2-10	LM 0.2-2	VLM <0.2	all
# of NIR sources	1	26	210	462	699
(those w/ X-ray)	1	21	139	268	268
# of NIR sources with NIR excess	0	12	45	74	131
(those w/ X-ray)	0	11	31	11	53

3.3. X-ray Spectral Analysis

142 X-ray sources with (1) S/N >10 and (2) X-ray counts > 50 were fitted with a thin-thermal plasma model. One-temperature (1T) model was applied for all sources first, then two-temperature (2T) model for those rejected by 1T model at a 5% significance level. 87 sources were fit with one-temperature and 41 were with two-temperature model.

3.4. X-ray Time-sliced Spectral Analysis

The 5 brightest sources that show flare-like time variability and have X-ray counts of more than 500 both in the flux-increase and quiescent states were conducted the above spectral analysis separately in the flux-increase and quiescent phases. Their light curves and spectra are shown in Fig.4, while the best-fit spectral parameters are in Table 2.

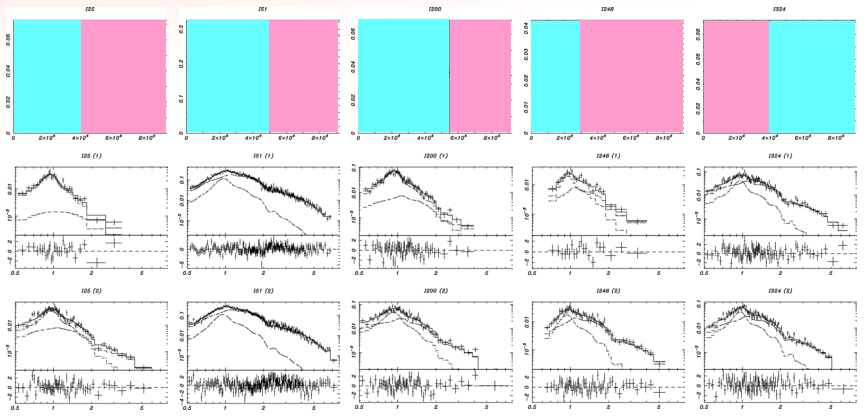

Fig.4 The results of the time-sliced spectroscopy of the 5 brightest variable sources. Upper panels show light curves (cyan; quiescent and magenta; flux increase), while middle and lower panels show the spectra and best-fit models of the former and latter slices.

Table 2 Best-fit parameters of the spectral fitting of each slice. All spectra are explained by two-temperature plasma model (higher and lower temperature component with blue and red colors).

object	slice	N_H (cm^{-2})	kT_1 (keV)	EM_1 (cm^{-3})	kT_2 (keV)	EM_2 (cm^{-3})
I25	1	0.0 (0.0-0.1)	9.7 (0.2-80.)	3.7 (1.0-9.1) e52	0.9 (0.2-1.0)	2.2 (0.1-2.5) e53
	2	0.0 (0.0-0.0)	4.8 (2.6-8.8)	1.8 (1.1-2.5) e53	1.0 (0.9-1.1)	2.8 (2.0-3.5) e53
I51	1	0.2 (0.2-0.2)	3.3 (3.0-3.6)	4.7 (4.3-25.) e54	1.0 (0.9-1.1)	1.2 (0.9-1.5) e54
	2	0.2 (0.2-0.2)	3.2 (3.0-3.5)	5.0 (4.6-25.) e54	0.9 (0.8-1.0)	1.1 (0.9-1.5) e54
I200	1	0.0 (0.0-0.1)	2.7 (1.7-9.4)	1.4 (0.7-2.0) e53	0.9 (0.8-0.9)	4.2 (3.5-5.0) e53
	2	0.0 (0.0-0.0)	2.3 (1.9-2.8)	4.3 (3.6-5.3) e53	0.8 (0.8-0.9)	2.7 (2.1-3.3) e53
I248	1	0.2 (0.0-0.8)	2.5 (0.5-27.)	2.0 (0.8-4.1) e53	0.9 (0.7-1.1)	1.9 (0.9-7.4) e53
	2	0.2 (0.1-0.3)	3.1 (2.5-3.8)	3.8 (3.1-4.4) e53	0.9 (0.7-1.0)	1.8 (1.2-2.9) e53
I324	1	0.1 (0.1-0.1)	3.2 (2.6-4.0)	8.7 (7.2-10.) e53	1.0 (0.8-1.1)	3.3 (2.2-4.6) e53
	2	0.1 (0.1-0.2)	2.6 (2.0-3.3)	6.7 (5.3-8.6) e53	1.0 (0.8-1.1)	3.8 (2.6-5.1) e53

4. Discussion

4.1. X-ray Emission Mechanisms among Mass Ranges

The X-ray detection rate of IM sources (80%; Table 1) is higher than the binary rate in Orion (15%)[5]. When restricted to those with NIR excess (=secure candidates of IM YSOs), all but one (11/12) emit X-rays. These indicate that *IM YSOs emit X-rays from themselves, not from their low-mass companion*.

We conclude that *the same X-ray emission mechanism works for IM, LM, and VLM sources* based on (1) the similar plasma temperature among IM-VLM sources, (2) L_x/L_{bol}=10^{-2}-10^{-5} (Fig.5), in contrast with L_x/L_{bol}=10^{-7} for the HM source with X-rays of stellar wind origin, and (3) a rough relation between L_x and M (Fig.6).

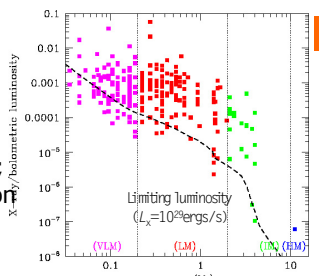

Fig.5 Relation between L_x/L_{bol} (y-axis) and M (x-axis) of NIR-identified X-ray sources. The limiting luminosity is shown with dashed curve.

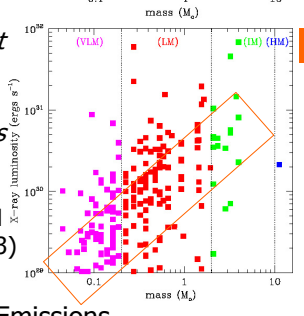

Fig.6 Relation between L_x (y-axis) and M (x-axis) of NIR-identified X-ray sources. A rough relation between L_x and M for VLM-IM sources is shown with a band.

4.2. Two-temperature Nature of Plasma Emissions

We propose that *X-ray emissions from IM-VLM YSOs are composed of the lower (k_BT=1 keV) and higher (k_BT=2-3 keV) temperature plasma with different mechanisms* based on (1) the bimodal structure in the temperature histogram (Fig.7a), with each peak corresponding to higher and lower component (Fig.7b), (2) different temporal behavior of the two components (Table 2), where the higher component increases its EM value toward flux increase while the lower component does not, (3) the temperature of almost all the sources with flare-like variability are 2-3 keV or above.

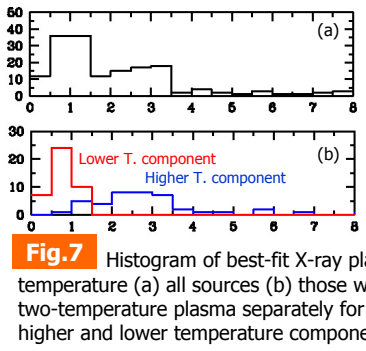

Fig.7 Histogram of best-fit X-ray plasma temperature (a) all sources (b) those with two-temperature plasma separately for higher and lower temperature components.

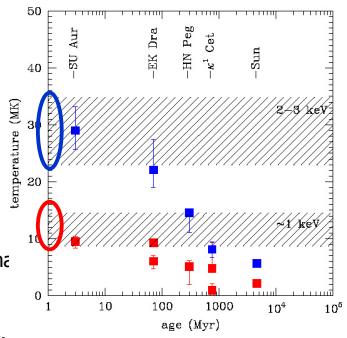

Fig.8 Age (x-axis) vs plasma temperature (y-axis; lower and higher temperature component with red and blue colors) of main sequence stars. The expected temperatures of each component at 1Myr (=the age of OMC-2/3) are shown with ellipses.

4.3. Origin of the Two-temperature Components

We finally propose that *the higher temperature component originates from flares while the lower component from stellar coronae* based on (1) the flux increases are attributable to higher component, (2) solar X-rays show two-temperature plasma, where higher is from flares and the lower is from the corona[7]. Other main sequence stars also show two- (or three-) temperature plasma[8][9], the temperatures of which increase as decreasing ages. The expected temperatures at 1 Myr (=the age of OMC-2/3) are 1 keV and 2-3 keV for lower and higher component, which agrees with our result. This may be because the rotational velocity decreases and the magnetic activity evolves inactive as stars age.

This works is a part of my Ph. D. thesis; "*A Multi-wavelength Study on the X-ray Emissions from Young Stellar Objects in Orion Molecular Cloud 2 and 3*", M. Tsujimoto 2003, Kyoto University, available at ftp://ftp.astro.psu.edu/pub/tsujimot/articles/phd.pdf. Hard copies are also available upon request.

References

[1] Chini, R. et al. 1997, ApJ, 474, L135
[2] Siess, L. et al. 2000, A&A, 358, 593
[3] Baraffe, I. et al. 1998, A&A, 337, 403
[4] Kukarkin, B. V. et al. 1971
[5] Padgett, D. L. et al. 1997, ApJ, 477, 705
[6] Yokoyama, T., & Shibata, K. 1998, ApJ, 494, L113
[7] Peres, G. et al. 2000, ApJ, 528, 537
[8] Guedel, M. et al. 1997, ApJ, 483, 947
[9] Skinner, S. L., & Walter, F. M. 1998, ApJ, 509, 761